Volume 1 | Number 1 | Jan 2013 | Pages 1–100

Catalysis
Science &
Technology

www.rsc.org/catalysis

ROYAL SOCIETY
OF CHEMISTRY

Journal Name

ARTICLE

Thermally Stable Gold/Alumina Aerogel Catalysts Prepared by a Simultaneous Synthesis Process for Solvent-Free Aerobic Benzyl Alcohol Oxidation

Z. Li,[a,b,c] YZ. Ji,[a] C. Cadigan[a] and R. M. Richards[a]*

Gold nanoparticles supported on an alumina aerogel have been prepared through a simultaneous synthesis process in which the formation of the gold nanoclusters capped with (3-aminopropyl)triethoxysilane (APTES) and the hydrolyzation/co-condensation of the APTES and aluminum alkoxide occur concurrently. The obtained gold nanoparticles are trapped in and physically protected by the framework of the alumina aerogel providing excellent thermal stability with no observable sintering at 650 °C. In the catalysis test for the solvent-free aerobic benzyl alcohol oxidation, this catalyst exhibits significantly better activity than reference gold/alumina aerogel catalysts prepared through a deposition precipitation and conventional wet impregnation methods, especially at high temperature.

1. Introduction

The catalytic performance of nanoparticles can be finely tuned either by their composition, which mediates electronic structure, or by their shape, which determines surface atomic arrangement and coordination. Beyond the exciting potential for tailoring catalysts, nanostructured materials introduce additional challenges to catalyst design. By being small and containing surface atoms of varying unsaturated valencies, nanoparticles of specific shape are more susceptible to morphological change in harsh chemical reaction environments.[1] Given the low melting points of nanoparticles as compared to their bulk counterparts, imparting stability to nanoscale catalysts (particularly gold) remains a challenge.[2]

Gold has long been considered an 'inert' metal. However, with the development of nanotechnology, it has been found that nano-scale gold is highly active for CO oxidation with great selectivity even at room temperature.[3] Thereafter, the field of gold nanocatalysts has been thoroughly studied and has rapidly become a promising system for hydrogenation[4] and epoxidation[5, 6] of alcohols[7, 8] and aldehydes[9] as well as oxidation and even aerobic oxidation of alkanes.[8, 10, 11] However, most applications of gold catalysts are performed under moderate conditions with relatively low temperatures (normally 80-120 °C). Working at higher temperatures, gold nanoparticles generally suffer from severe sintering and loss of activity, greatly limiting the practical application of gold catalysts.[12] In fact, the sintering of gold catalysts also happens during the moderate calcination (250-350 °C) process of catalyst preparations. The thermal stability of gold catalysts can be somewhat improved by removal of the chloride ions in the catalysts or by using expensive chloride-free gold precursors.[13] Numerous efforts have been made to address this problem by

modifying the surface of gold nanoparticles or the surface of the supporting materials. One promising approach is to physically trap the gold catalysts in the rigid structure of metal oxides.[14] Very recently, atomic layer deposition (ALD) has been used to stabilize nanoporous gold with a thin layer of Al_2O_3, greatly improving the thermal stability of the gold.[15] Futhermore, in our previous work, we have reported gold catalysts intercalated in the walls of mesoporous silica with improved thermal stability.[11, 16]

In this work, we have improved the thermal stability of Au/Al_2O_3 catalysts by simultaneously hydrolyzing/condensing aluminum alkoxide and reducing the gold precursor in the presence of (3-aminopropyl)triethoxysilane (APTES) as a linking agent. The obtained catalyst can endure calcination temperatures up to 650 °C while maintaining excellent catalytic activity at 160 °C in the solvent-free aerobic benzyl alcohol oxidation. Au/Al_2O_3 catalysts prepared by a conventional impregnation method and a deposition-precipitation (DP) method have also been tested as controls.

2. Results and discussion

2.1 Synthesis of Au/Al_2O_3 catalyst

An ultrastable Au/Al_2O_3 catalyst was prepared by a simultaneous synthesis method, during which the reduction of Au^{3+} and the hydrolyzation/condensation of the aluminum alkoxide took place at the same time. APTES, well-known for its affinity to gold nanoparticles, was used as a linking agent. As shown in **Figure 1**, the as-formed gold nanoclusters, bonded to the (NH_2-) end of APTES, were further stabilized during the co-condensation of ethoxy groups and concurrent sol-gel processes occurring with aluminum alkoxide. The co-condensation process prevents the gold clusters from further growth and results in a uniform structure with tiny gold

particles trapped in the framework of Al_2O_3 (with a small amount of SiO_2 from APTES) after supercritical drying and calcination at 500 °C. The nomenclature $Au/SiO_2@Al_2O_3$ is used henceforth in this manuscript for this catalyst system. As a control, a pure Al_2O_3 aerogel has been prepared under the same conditions without addition of APTES and gold precursor. The obtained Al_2O_3 aerogel was used as supporting material to prepare the reference catalyst by impregnation method (termed Au/Al_2O_3 herein).
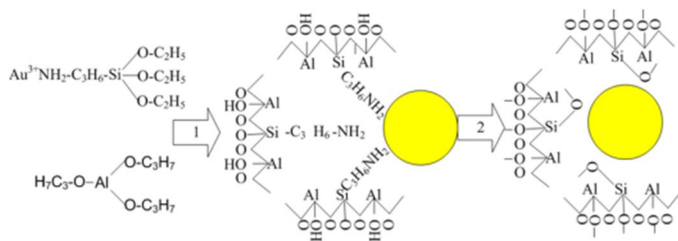

Figure 1 The schematic illustration of the simultaneous synthesis process of $Au/SiO_2@Al_2O_3$. The arrow marked as '1' signifies the reduction of gold and hydrolysis and condensation of aluminum alkoxide and APTES; the arrow marked as '2' signifies the 5 hour calcination process at 500 °C.

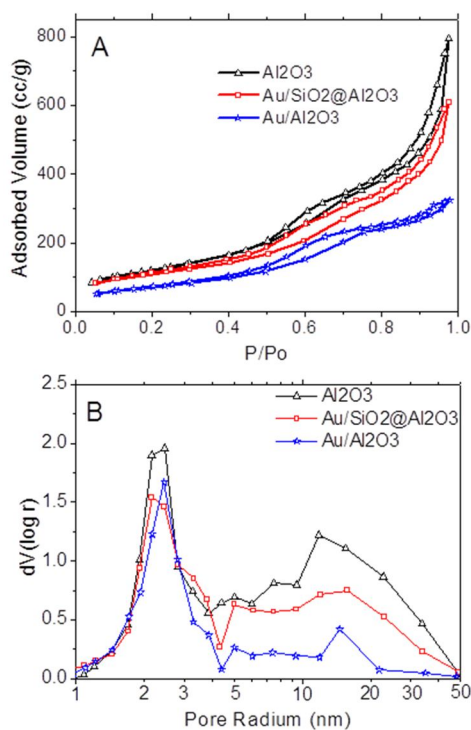## 2.2 Porous texture and chemical features of the catalyst systems

Figure 2. Nitrogen adsorption/desorption isotherms at -196 °C (A) and BJH pore-size distribution (B) of $Au/SiO_2@Al_2O_3$, Au/Al_2O_3 and Al_2O_3 aerogel.

Surface area and porosity were analyzed by N_2-adsorption at -196 °C. As shown in **Figure 2A**, Al_2O_3 aerogel, $Au/SiO_2@Al_2O_3$ and Au/Al_2O_3 all exhibit type IV isotherms with H1-type hysteresis loops at P/P_0=0.5-1.0. This is characteristic of a combined pore system with mostly small mesopores with some larger mesopores. Compared with the other two, the hysteresis loops of Au/Al_2O_3 are less developed

at high pressure (P/P_0=0.75-1.0), indicating fewer large mesopores in the sample. This difference is also observed in the pore size distribution plots (**Figure 2B**) calculated by the Barrett-Joyner-Halenda (BJH) model with a sharp peak centered at 2.4 nm (pore radius) in all three samples. The pores of this size are formed by the packing of the Al_2O_3 nanoparticles. There are also broad peaks in the range of 5-50 nm, which correspond to the large pores formed during formation of the Al_2O_3 gel. However, in the case of Au/Al_2O_3, this peak is significantly smaller than that of other samples, suggesting part of the pore structure formed in gelation was destroyed in the conventional wetness impregnation preparation of gold catalysts. As listed in **Table 1**, $Au/SiO_2@Al_2O_3$ has a large surface area (384 m^2/g), slightly lower than that of pure Al_2O_3 aerogel (441 m^2/g), indicating that the gold nanoparticles formed in the simultaneous deposition process did not influence the formation of the sol-gel pore structure. The impregnation and calcination processes resulted in a loss of more than 40% of the surface area of the aerogel. In fact, the effect of solvent on the support materials is an unavoidable factor in most post treatment methods to prepare heterogeneous catalysts via deposition-precipitation (DP) or wetness impregnation. The gold content of $Au/SiO_2@Al_2O_3$ and Au/Al_2O_3 are 1.1% and 1.0% respectively as measured by inductively coupled plasma mass spectrometry (ICP-MS) analysis. The $Au/SiO_2@Al_2O_3$ catalyst also contains around 5% SiO_2, which is from APTES.

Table 1. N_2-Adsorbption data and Au content of different samples.

Sample	Calcine [℃]	S_{BET} [a] [m^2/g]	V_{total} [b] [cm^3/g]	Au^c [wt%]	Au Size [d] [nm]
Al_2O_3	500	441	1.08		
$Au/SiO_2@Al_2O_3$	500	384	1.07	1.1	3-5 (spheres)
Au/Al_2O_3	350	252	1.03	1.0	3-30 (irregular)

[a] The surface area S_{BET} is calculated by a multi point BET method (7 points were selected in the range of P/P_o=0.1-0.3); [b] total pore volume; [c] weight content of Au in catalysts, determined by ICP-MS analysis; [d] the size of gold nanoparticles is determined by TEM.

2.3 Structure and morphology of gold nanoparticles

Considering that the $Au/SiO_2@Al_2O_3$ catalyst was calcined at 500 °C, we are extremely interested in the morphology of the gold nanoparticles: whether or not they agglomerated like the typical gold nanoparticles supported on Al_2O_3.[17, 18] In order to increase the contrast between gold nanoparticles and the alumina, Scanning Transmission Electronic Microscopy (STEM-Dark field mode) was utilized to study the morphology and distribution of gold nanoparticles supported on alumina aerogel. **Figure 3A** shows an overview of the $Au/SiO_2@Al_2O_3$ catalyst, where the uniform gold nanoparticles are evenly distributed on the alumina support. Those gold nanoparticles show a sphere-like structure and are 3-5 nm in diameter (**Figure 3B**). No agglomeration of gold nanoparticles was observed after calcination at 500 °C. The selected area dispersive X-ray (SAEDX) analysis shown in **Figure 3C** indicates the existence of Si (from APTES), Au, Al, O and C (from the carbon film on TEM grids). To evaluate the thermal stabilities of the $Au/SiO_2@Al_2O_3$ catalyst, the sample was also calcined at 650 ℃ and 750 ℃. As seen in **Figure 3D,** the gold nanoparticles retain uniform size and are well dispersed on the support after calcination at 650 °C. Furthermore, the high

magnification image shown in the inset reveals that the particles are only slightly larger at 5-10 nm. Even after calcination at 750 °C, about half of the gold particles are still around 5 nm in size, but some larger agglomerations begin to appear at this calcination condition (**Figure 3E**). From the inset, larger particles around 20-30 nm can be observed.
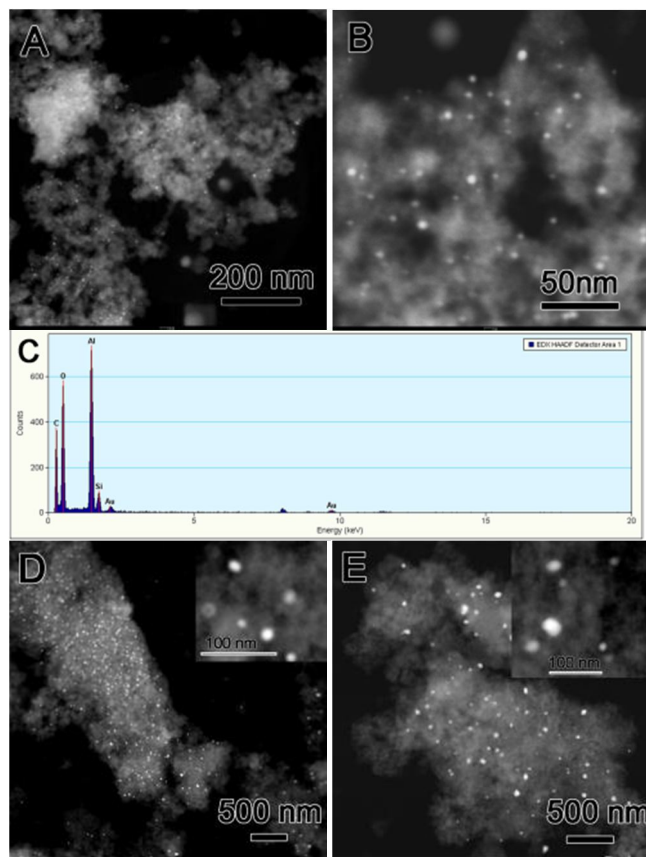

Figure 3. HAADF-STEM images of Au/SiO$_2$@Al$_2$O$_3$ catalyst (A, B) and the EDX analysis at the selected area (C); HAADF-STEM images of Au/SiO$_2$@Al$_2$O$_3$ catalyst calcined at 650 °C (D) and 750 °C (E).

For comparison, **Figure 4** shows the Au/Al$_2$O$_3$ catalyst prepared by the wet impregnation method. The alumina support shows a similar morphology with that of Au/SiO$_2$@Al$_2$O$_3$ and is typical of an alumina aerogel. However, the supported gold shows various shapes and sizes with some 3-5 nm spheres as well as significant agglomerations (some reaching 30 nm). Given the reference catalyst was calcined at a much lower temperature (350 °C), it is inferred that the simultaneous synthesis method yields a gold catalyst with significantly improved thermal stability than conventional gold catalysts.
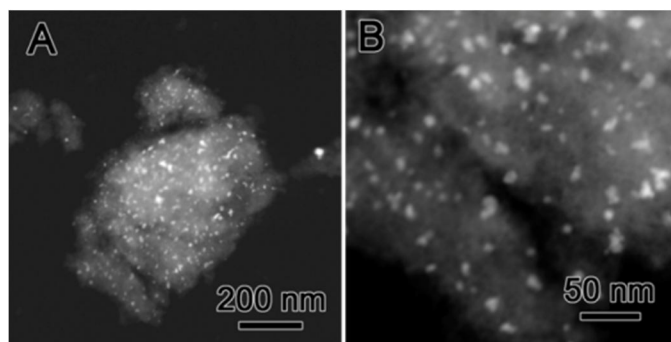

Figure 4. HAADF-STEM images of Au/Al$_2$O$_3$.

Figure 5A shows the X-ray diffraction pattern of the Au/SiO$_2$@Al$_2$O$_3$ and Au/Al$_2$O$_3$ samples. The Al$_2$O$_3$ supports of both samples exhibit very broad diffraction peaks indicating that they are composed of very fine nanoparticles. However, the gold peak is not observable in any of the samples. That is mainly because the two strongest diffraction peaks of Au, namely (111) at 38.18° and (200) at 44.39° will be relatively small given the low Au concentration (around 1 wt%) and the truly nanoscale size of Au particles. Additionally, the small Au peaks can be concealed by the larger broad peaks of Al$_2$O$_3$ at similar positions (35.14° and 43.36°). However, the broad diffraction peak of Al$_2$O$_3$ at 35.14° shows a small shoulder at around 38°, which might be attributed to the Au(111) diffraction. It is well-known that the surface plasma resonance (SPR) of gold nanoparticles is closely related to their particle size.[19] Diffuse-reflectance UV-vis spectra were used to investigate the SPR of the two catalysts (**Figure 5B**). Both catalysts show a sharp SPR peak in the range of 500-600 nm as evidence that the gold particles are nanoscale in size. Furthermore, the SPR peak of Au/SiO$_2$@Al$_2$O$_3$ (519 nm) was slightly blue shifted as compared to Au/Al$_2$O$_3$, indicating that the Au particles in Au/SiO$_2$@Al$_2$O$_3$ are slightly smaller.
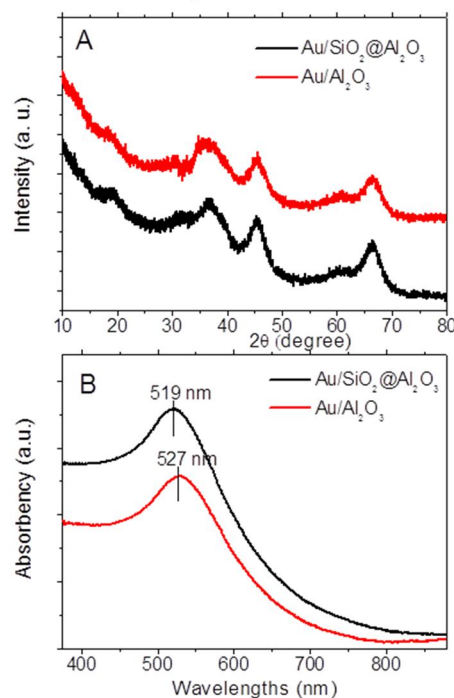

Figure 5. XRD spectra (A) and diffuse-reflectance UV-vis spectra (B) of Au/SiO$_2$@Al$_2$O$_3$ and Au/Al$_2$O$_3$ catalysts.

T (^{o}C)	Catalysts	Conversion	Selectivity (mol. %)
160	Al$_2$O$_3$	6.67	80.97
	Au/SiO$_2$@Al$_2$O$_3$	21.90	72.32
	Au/Al$_2$O$_3$ DP	8.99	89.33
	Au/Al$_2$O$_3$	10.42	75.96

[a] The selectivity to benzaldehyde.

2.4 Catalytic performance of ultrastable Au/SiO$_2$@Al$_2$O$_3$ catalysts

The oxidation of benzyl alcohol, as a model reaction for primary alcohol oxidation,[20] was used in this work to study the activity of the Au/SiO$_2$@Al$_2$O$_3$ prepared by simultaneous synthesis. All reactions were performed in the absence of solvent with a 6 h reaction time. No detectable benzene or toluene was produced in the reactions. The byproduct is mainly benzyl benzoate rather than benzoic acid, indicating either the immediate esterification between benzoic acid and benzyl alcohol, or that oxidation occurs directly on the hemiacetal [PhCH(OH)OCH$_2$Ph] formed from benzaldehyde and benzyl alcohol without ever forming benzoic acid.[5, 21] Comparing the performance of Au/SiO$_2$@Al$_2$O$_3$, Au/Al$_2$O$_3$, Au/Al$_2$O$_3$ DP and pure Al$_2$O$_3$ (to evaluate the contribution of supporting material), it can be inferred that the gold nanoparticles have minimal contributions to the overall conversion at 100 °C (**Table 2**). The activity of gold nanoparticles increases with temperature, but Au/SiO$_2$@Al$_2$O$_3$ showed no significant advantage over Au/Al$_2$O$_3$ at 120 °C and 140 °C indicating that the catalysts work similarly under those moderate conditions. However, Au/SiO$_2$@Al$_2$O$_3$ gives a conversion of 21.90% at 160 °C, more than two times the conversion demonstrated by Au/Al$_2$O$_3$ (10.42%) with similar selectivity to benzldehyde. Indeed, higher conversion is always desirable as long as the catalyst can handle the high temperature and still give reasonable selectivity. The Au/Al$_2$O$_3$ DP catalyst had the lowest activities among the three Au catalysts at higher temperatures, but the highest selectivity to benzaldehyde as reaction temperature elevates to 160 °C.

To determine the Au leaching of our Au/Al$_2$O$_3$ catalyst, the solution after catalytic reaction was collected and Au composition determined by ICP. Results indicated that at 100 °C, 0.412% of Au was leached after reaction, the leaching of Au slightly increased to 0.466% at 120°C and finally reached 0.523% for reaction at 160°C. Au leaching is minor in all catalytic reactions, even at a high temperature of 160 °C, suggesting a good thermal stability of simultaneous synthesized Au/Al$_2$O$_3$ catalyst

Table 2 Comparative data for solvent-free aerobic oxidation of benzyl alcohol. The oxidation was carried out by bubbling oxygen into the reaction mixture (5 ml benzyl alcohol and 5 mg catalysts) at different temperatures. Results were obtained after 6 h of reaction.

T (^{o}C)	Catalysts	Conversion	Selectivity (mol. %)
100	Al$_2$O$_3$	1.32	82.31
	AuSiO$_2$@Al$_2$O$_3$	1.76	77.39
	Au/Al$_2$O$_3$ DP	2.59	61.06
	Au/Al$_2$O$_3$	2.03	81.01
120	Al$_2$O$_3$	2.87	85.22
	Au/SiO$_2$@Al$_2$O$_3$	6.09	88.52
	Au/Al$_2$O$_3$ DP	3.55	67.28
	Au/Al$_2$O$_3$	5.90	84.72
140	Al$_2$O$_3$	3.08	83.24
	Au/SiO$_2$@Al$_2$O$_3$	7.40	83.51
	Au/Al$_2$O$_3$ DP	6.16	84.61
	Au/Al$_2$O$_3$	6.77	82.78

We attribute the good performance of Au/SiO$_2$@Al$_2$O$_3$ to its thermal stability. In fact, gold nanoparticles are generally highly mobile on Al$_2$O$_3$ surfaces due to the Au-Al$_2$O$_3$ bond energy being substantially weaker than that of Au-TiO$_2$[17] and small gold Au nanoparticles may be more mobile than gold atoms.[18] Thus, the agglomeration of gold nanoparticles is problematic for the Au/Al$_2$O$_3$ system, especially when HAuCl$_4$ (the most common gold precursor) is involved in the preparation, because the chloride ions can significantly accelerate the agglomeration process.[22] **Figure 4** clearly shows the aggregation of gold deposited on Al$_2$O$_3$ by a typical wetness impregnation method calcined at 350 °C in air. Though the oxidation of benzyl alcohol is run at relatively low temperatures, the agglomeration may be even higher due to the influence of the hot liquid. As shown in **Figure 1**, in the simultaneous synthesis process, the reduction of gold takes place at the same time as the hydrolyzation and condensation of metal alkoxide and APTES. Three additional factors to stabilize the gold nanoparticles can be expected from this process, i) the amino head of APTES can promote even distribution of Au^{3+} by anchoring it; ii) when gold nanoparticles form, the SiO$_2$ condenses with the Al$_2$O$_3$ support and due to the well-known affinity between its amino head group and gold surface, the APTES can increase the interface between gold and Al$_2$O$_3$ to stabilize gold nanoparticles; iii) although the APTES functional group was damaged after calcinations at 500 °C, the enhanced interfaces are still there to hamper the mobility of gold nanoparticles. To confirm the stability of the catalysts in the reaction, we have acquired bright-filed TEM images of Au/SiO$_2$@Al$_2$O$_3$ before and after reaction. As shown in **Figure 6**, no observable changes in particle morphology or size can be found. Histogram indicated that size of Au particles in the materials both before and after reaction evenly distributed between the range of 2.5 – 5.5 nm, with peaking at 4.5 – 5 nm.
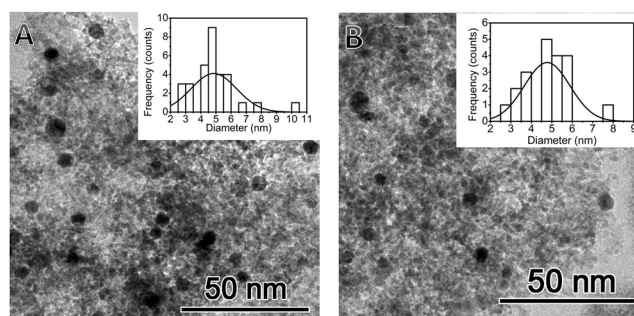

Figure 6. Bright-field TEM images of Au/SiO$_2$@Al$_2$O$_3$ catalyst before (A) and after (B) reaction at 120 ^{o}C.

3. Experimental
3.1 Materials and instruments
Hydrogen tetrachloroaurate (HAuCl$_4$•3H$_2$O, 99.99%), Cetyltrimethylammonium bromide (CTAB, 99%), isopropanol (99.5%) and 3-amimopropyl-triethoxysilane (APTES) were obtained from Sigma-Aldrich. Freshly calcined (550 °C) molecular sieves (4Å) were added to the isopropanol to further

remove any residual water. All other reagents were procured from Aldrich and used as received. Ultrapure deionized water (Continental Water Systems) was used throughout the experiments. Transmission electron microscopy (TEM) studies were performed on a FEI Tecnai F20 S-Twin operated at 200 kV. The samples were prepared by spreading an ethanolic suspension on carbon coated copper grids. BET and isothermal measurements were performed on a Quantachrome Nova 4000e. X-ray diffraction was acquired on a Siemens D 5000 diffractometer (Cu Ka, λ=1.5406A). The diffuse reflectance UV-vis spectra were recorded on a UV4 (Unicom) spectrophotometer. Calcination was performed in a tubular furnace with a ramping rate of 3 °C per minute.

3.2 Synthesis of Au/SiO₂@Al₂O₃

Hydrogen tetrachloroaurate was first dissolved in distilled water and then transferred into toluene with the help of a phase transfer agent (CTAB). Typically, an aqueous solution of hydrogen tetrachloroaurate (5ml, 0.02M) was added to the mixture of CTAB (50 mg) and toluene (10 ml) under vigorous stirring. After 2 h, tetrachloroaurate was completely transferred into the toluene phase to form a 0.01 M solution (Solution A) and the water phase became colorless. In another flask, 1.0 g of aluminium triisopropoxide was dissolved in 50 ml pretreated anhydrous isopropanol and then 50 ml anhydrous toluene was added and stirring was maintained for 5 h to form a transparent solution. 2 ml of solution A and 0.05 ml APTES was added to this clear solution. After stirring for one more hour, 15 ml isopropanol solution containing 0.2 ml water and 5 mg sodium borohydride was added dropwise to the flask over 30 min. The gelation process was performed by maintaining stirring for 24 h at room temperature. The Al₂O₃ gel doped with gold nanoparticles was washed three times by centrifuging, re-dispersing in a 100 ml solution of isopropanol and toluene (1:1 by volume) and drying by supercritical treatment at 265 °C in a Parr autoclave. The obtained powder was calcined at 500 °C for 5 h under the protection of argon. The Al₂O₃ aerogel was prepared under the same conditions without adding the gold precursor, APTES and sodium borohydride.

3.3 Synthesis of reference Au/Al₂O₃ catalyst

The Au/Al₂O₃ sample was prepared following a reported method.[23] In a typical experiment, 1.0 g of Al₂O₃ aerogel was stirred in 50 ml 9.7 mM chlorauric acid for 5 h at 70 °C. Then the powder was filtered and re-suspended in 50 ml DI water. After refluxing at 70 °C for 1 h, the powder was filtered again and calcined at 350 °C for 5 h. The final product was a light pink powder, denoted as Au/Al₂O₃.

3.4 Synthesis of reference Au/Al₂O₃ DP catalyst

The preparation of Au/Al₂O₃ DP follows literature reports.[24] Typically, a solution of HAuCl₄.3H₂O (10 mg) in 100 ml of DI water was heated to 80 °C and adjusted to pH=8.5 with NaOH. Al₂O₃ aerogel (0.5 g) was then added to the solution under vigorous stirring while the pH was still maintained at 8.5 using NaOH and HCl. Once the pH stabilized, the mixture was stirred at 80 °C for 2 h. The precipitation was collected, washed several times and dried at 100 °C. The obtained powder was calcined at 450 °C for 4 h and denoted as Au/Al₂O₃ DP.

3.5 Benzyl alcohol oxidation

The liquid phase oxidation of benzyl alcohol over the supported Au catalysts were carried out in a magnetically stirred 25 ml three-neck flask with oil bath heating and reflux condenser, under the following general reaction conditions: reaction mixtures = 5 ml benzyl alcohol + 5 mg catalyst, reaction time = 6 h, temperature varied from 100 °C to 160 °C in different experiments, 99.9% oxygen was bubbled into the reaction mixture at the rate of approximately 2 ml/min. After the reaction, the reaction mixture was filtered and the liquid phase from was analyzed by a gas chromatograph equipped with a flame ionization detector, using N₂ as a carrier gas. The reaction products and unconverted reactants were identified by comparison with authentic standard samples. The conversion and product selectivity were calculated as follows: conversion (%) = (moles of reactant converted) / (moles of reactant in feed) X 100 and product selectivity (%) = (moles of product formed) / (moles of reactant converted).

4. Conclusions

In this work, we demonstrate a simultaneous synthesis process which can significantly increase the thermal stability of gold/alumina aerogel catalysts by increasing the Au-Al₂O₃ interface and trapping gold nanoparticles in the framework of an alumina aerogel. No agglomeration was found even after 5 h calcination at 650 °C. Furthermore, the Au/Al₂O₃ prepared by this process demonstrated superior performance at high temperatures than that of systems prepared by deposition precipitation and wetness impregnation methods.

Acknowledgements

Notes and references

[a] Department of Chemistry and Geochemistry, Colorado School of Mines, 1500 Illinois St. Golden, CO, 80401 USA. Fax: 303 273 3629; Tel: 303 273 3612; E-mail: rrichard@mines.edu.

[b] Chemical and Materials Engineering, University of Alberta, 9107 116 St., Edmonton, AB, T6G 2V4, Canada..

[c] National Institute for Nanotechnology (NINT), NRC, 11421 Saskatchewan Dr., Edmonton, AB, T6G 2M9,Canada.

1   A. Leyva-Perez and A. Corma, *Angew. Chem. Int. Ed.*, 2012, **51**, 614.
2   M. Rudolph and A. S. K. Hashmi, *Chem. Soc. Rev.*, 2012, **41**, 2448.
3   M. Haruta, S. Tsubota, T. Kobayashi, H. Kageyama, M. J. Genet and B. Delmon, *J. Catal.*, 1993, **144**, 175; M. Haruta, N. Yamada, T. Kobayashi and S. Iijima, *J. Catal.*, 1989, **115**, 301.
4   S. Bhattacharjee, D. M. Dotzauer and M. L. Bruening, *J. Am. Chem. Soc.*, 2009, **131**, 3601;   A. Corma and P. Serna, *Science*, 2006, **313**, 332;   V. I. Parvulescu, V. Parvulescu, U. Eudruschat, G. Filoti, F. E. Wagner, C. Kubel and R. Richards, *Chem. Eur. J.*, 2006, **12**, 2343.
5   V. R. Choudhary and D. K. Dumbre, *Top. Catal.*, 2009, **52**, 1677.
6   A. Zwijnenburg, M. Makkee and J. A. Moulijn, *Appl. Catal., A*, 2004, **270**, 49;   A. Zwijnenburg, M. Saleh, M. Makkee and J. A. Moulijn, *Catal. Today*, 2002, **72**, 59; G. Mul, A. Zwijnenburg, B. van der Linden, M. Makkee and J. A. Moulijn, *J. Catal.*, 2001, **201**, 128.

7   K. M. Kosuda, A. Wittstock, C. M. Friend and M. Baumer, *Angew. Chem. Int. Ed.*, 2012, **51**, 1698;   P. Rodriguez, Y. Kwon and M. T. M. Koper, *Nat. Chem.*, 2012, **4**, 177;   H. F. Guo, A. Al-Hunaiti, M. Kemell, S. Rautiainen, M. Leskela and T. Repo, *Chemcatchem*, 2011, **3**, 1872;   J. C. Hu, L. F. Chen, K. K. Zhu, A. Suchopar and R. Richards, *Catal. Today*, 2007, **122**, 277;   D. I. Enache, J. K. Edwards, P. Landon, B. Solsona-Espriu, A. F. Carley, A. A. Herzing, M. Watanabe, C. J. Kiely, D. W. Knight and G. J. Hutchings, *Science*, 2006, **311**, 362;   Z. Li, C. V. Ciobanu, J. C. Hu, J. P. Palomares-Baez, J. L. Rodriguez-Lopez and R. Richards, *PCCP*, 2011, **13**, 2582.

8   H. Tsunoyama, Y. M. Liu, T. Akita, N. Ichikuni, H. Sakurai, S. H. Xie and T. Tsukuda, *Catal. Surv. Asia*, 2011, **15**, 230.

9   A. Corma and M. E. Domine, *Chem. Commun.*, 2005, 4042;   M. Besson and P. Gallezot, *Catal. Today*, 2000, **57**, 127.

10   J. M. Thomas, R. Raja, G. Sankar and R. G. Bell, *Nature*, 1999, **398**, 227;   H. Zhao, J. C. Zhou, H. Luo, C. Y. Zeng, D. H. Li and Y. J. Liu, *Catal. Lett.*, 2006, **108**, 49;   R. Zhao, D. Ji, G. M. Lv, G. Qian, L. Yan, X. L. Wang and J. S. Suo, *Chem. Commun.*, 2004, 904.

11   K. K. Zhu, J. C. Hu and R. Richards, *Catal. Lett.*, 2005, **100**, 195.

12   F. Boccuzzi, A. Chiorino, M. Manzoli, P. Lu, T. Akita, S. Ichikawa and M. Haruta, *J. Catal.*, 2001, **202**, 256;   E. D. Park and J. S. Lee, *J. Catal.*, 1999, **186**, 1.

13   S. Ivanova, W. Pitchon, Y. Zimmermann and C. Petit, *Appl. Catal., A*, 2006, **298**, 57.

14   P. M. Arnal, M. Comotti and F. Schüth, *Angew. Chem.*, 2006, **118**, 8404.

15   M. M. Biener, J. Biener, A. Wichmann, A. Wittstock, T. F. Baumann, M. Baumer and A. V. Hamza, *Nano Lett.*, 2011, **11**, 3085.

16   L. F. Chen, J. C. Hu and R. Richards, *J. Am. Chem. Soc.*, 2009, **131**, 914;   X. Wang, L. F. Chen, M. Shang, F. Lin, J. C. Hu and R. M. Richards, *Nanotechnology*, 2012, **23**.

17   S. Lee, C. Y. Fan, T. P. Wu and S. L. Anderson, *J. Phys. Chem. B*, 2005, **109**, 11340.

18   J. Carrey, J. L. Maurice, F. Petroff and A. Vaures, *Surf. Sci.*, 2002, **504**, 75.

19   S. Eustis and M. El-Sayed, *J. Phys. Chem. B*, 2005, **109**, 16350.

20   N. Dimitratos, J. A. Lopez-Sanchez and G. J. Hutchings, *Chem. Sci.*, 2012, **3**, 20.

21   V. R. Choudhary, R. Jha and P. Jana, *Green Chem.*, 2007, **9**, 267;   V. R. Choudhary, A. Dhar, P. Jana, R. Jha and B. S. Uphade, *Green Chem.*, 2005, **7**, 768.

22   J. H. Yang, J. D. Henao, C. Costello, M. C. Kung, H. H. Kung, J. T. Miller, A. J. Kropf, J. G. Kim, J. R. Regalbuto, M. T. Bore, H. N. Pham, A. K. Datye, J. D. Laeger and K. Kharas, *Appl. Catal., A*, 2005, **291**, 73.

23   J. T. Calla and R. J. Davis, *Ind. Eng. Chem. Res.*, 2005, **44**, 5403.

24   V. R. Choudhary and D. K. Dumbre, *Catal. Commun.*, 2009, **10**, 1738.

Gold nanoparticles physically trapped in the framework of alumina aerogel exhibit excellent thermal stability and catalytic activity at high temperature.